



SWIFT-XRT-CALDB-09

Release Date: 2014-Jun-10

Prepared by: Andrew Beardmore¹, Julian Osborne¹,
Claudio Pagani¹, Sergio Campana²

Document revision date: 2014-Jul-02

Revision: 19

Revised by: Andrew Beardmore

Affiliation: ¹ University of Leicester, ² INAF-OAB

SWIFT XRT CALDB RELEASE NOTE

SWIFT-XRT-CALDB-09:

Epoch Dependent $V_{SS} = 6\text{ V}$ Response Matrices

Table P1: Files to be released:

Filename	Mode	Grade	Substrate [†] voltage (V)	Start Date	End Date
swxpc0to12s6_20090101v014.rmf swxpc0to4s6_20090101v014.rmf swxpc0s6_20090101v014.rmf	PC	0 – 12 0 – 4 0	6	2009-Jan-01	2010-Dec-31
swxpc0to12s6_20110101v014.rmf swxpc0to4s6_20110101v014.rmf swxpc0s6_20110101v014.rmf	PC	0 – 12 0 – 4 0	6	2011-Jan-01	2012-Dec-31
swxpc0to12s6_20130101v014.rmf swxpc0to4s6_20130101v014.rmf swxpc0s6_20130101v014.rmf	PC	0 – 12 0 – 4 0	6	2013-Jan-01	—
swxwt0to2s6_20090101v015.rmf swxwt0s6_20090101v015.rmf	WT	0 – 2 0	6	2009-Jan-01	2010-Dec-31
swxwt0to2s6_20110101v015.rmf swxwt0s6_20110101v015.rmf	WT	0 – 2 0	6	2011-Jan-01	2012-Dec-31
swxwt0to2s6_20130101v015.rmf swxwt0s6_20130101v015.rmf	WT	0 – 2 0	6	2013-Jan-01	2013-Dec-11
swxwt0to2s6_20131212v015.rmf swxwt0s6_20131212v015.rmf	WT	0 – 2 0	6	2013-Dec-12	—

[†] The substrate voltage was permanently raised from $V_{SS} = 0\text{ V}$ to $V_{SS} = 6\text{ V}$ on 2007-Aug-30 (see below).

Scope of Document

This document describes the release of further epoch dependent *Swift*-XRT Photon Counting (PC) mode and Windowed Timing (WT) redistribution matrix files (RMFs), appropriate for substrate voltage 6V (i.e. $V_{ss} = 6\text{ V}$) data taken after 2007-Aug-30, which track the evolution of the CCD trap-corrected spectral resolution.

Introduction

The XRT effective area is made up of three main components: the mirror effective area, the filter transmission and the CCD quantum efficiency (QE). The QE is included directly in the redistribution matrix files (RMFs) while the ancillary response files (ARFs) contain the mirror effective area and the filter transmission.

Observation-specific ARF files are produced by the XRTMKARF task (part of the XRTDAS-HEADAS software). This task corrects the nominal (on-axis, infinite extraction region) ARF file from the CALDB for the effects of telescope vignetting and, optionally (*psfflag=yes*), for PSF losses incurred when finite sized extraction regions are used in point source analysis. Additional corrections for CCD defects (caused by ‘bad columns’ or ‘hot-pixels’) can be made with the inclusion of an exposure map (with the option *expofile=filename.img*), which can automatically be generated by the data analysis pipeline. The task can also generate ARFs for extended sources (option *extended=yes*), such as clusters of galaxies or supernova remnants.

As well as accounting for the CCD QE, the RMFs model the response of the detector to incident X-rays and are mode, grade and epoch dependent.

Motivation behind this release

Over time, the accumulated radiation dose and high-energy proton interactions cause damage to the CCD (in the imaging area, the store frame area and the serial register) resulting in a build-up of charge traps (i.e. faults in the Si crystalline structure of the CCD which hold onto some of the charge released during an X-ray interaction). The deepest traps are responsible for the strongest spectral degradation, causing a monochromatic line to show a more pronounced low energy wing. The most serious of these charge traps can cause a loss of up to $\sim 600\text{ eV}$ at 6 keV and $\sim 300\text{ eV}$ at 1.856 keV from the incident X-ray energy, although typical values are very much smaller.

For observations taken on or after 2007-Sep-01, we have mapped the location and depths of the deepest traps on the CCD and updated the *Swift*-XRT XRTCALCPI software task to provide a trap specific energy scale reconstruction (see the gain file release note SWIFT-XRT-CALDB-04.v10 and later for details and caveats).

The application of such trap corrections help restore the spectral resolution (i.e. intrinsic line Full Width at Half Maximum [FWHM]) of the detector — improvements in FWHM from 180 eV in PC (225 eV in WT) at 1.86 keV in early 2009 to approximately 135 eV (for both modes) are seen for the Tycho SNR. However, by 2013, the trap corrected FWHM at 1.86 keV had increased to 150 eV in PC mode and 170 eV in WT mode, indicating that further spectral degradation has occurred as the trap density continues to increase.

Also, observations of the low-energy, line rich source SNR 1E0102.2–7219, with its IACHEC reference model (Plucinsky et al., 2012, SPIE, 8443, 12), indicate that further epoch dependent RMF kernel broadening is required beyond that provided by the $V_{ss} = 6\text{ V}$ RMFs released on 2013-Dec-20 (described in SWIFT-XRT-CALDB-09.v18).

Additionally, the strength of the redistribution tail seen in WT data is found to be dependent on the value of the event threshold used to calculate the RMF. The WT event threshold was set to 80 DN onboard shortly after launch. However, the gradual increase of the CCD Charge Transfer Inefficiency (CTI) and the evolution in the distribution of deep charge traps means that, in real energy terms, the threshold has increased slowly with time. For example, in 2005-January the threshold occurred at 210 eV whereas in 2013-November it was close to $\sim 320\text{ eV}$. To counter this increase, the XRT team lowered the onboard WT threshold to 60DN ($\sim 260\text{ eV}$) on 2013-December-11. As the charge traps appear shallower in PC mode and the effective event threshold has remained below 300 eV (reaching $\sim 280\text{ eV}$ on 2013-Dec-07), the threshold has not been changed in this mode

Table 1: CCD Monte-Carlo simulator inputs and RMF minimum usable energy.

Epoch	EN (e^-)*	CTI _s [†]	CTI _p [‡]	Threshold (eV) [◇]		Minimum E (keV) [♣]	
				PC	WT	PC	WT
2007-Sep-01	7.5	3.5×10^{-5}	3.5×10^{-5}	220	220	0.30	0.30
2009-Jan-01	8.5	5.0×10^{-5}	5.0×10^{-5}	240	255	0.30	0.33
2011-Jan-01	9.0	6.0×10^{-5}	6.0×10^{-5}	255	270	0.30	0.35
2013-Jan-01	9.5	6.0×10^{-5}	1.0×10^{-4}	255	290	0.30	0.40
2013-Dec-12	9.5	6.0×10^{-5}	1.0×10^{-4}	—	270	0.35	0.30

* electronic noise (σ); [†] serial CTI; [‡] parallel CTI; [◇] MC input threshold — NB the effective threshold is $\sim (1 - CTI_s)^{-300}(1 - CTI_p)^{-900} \times$ higher; [♣] approximate lowest usable energy when fitting

Epoch Dependent $V_{ss} = 6$ V RMFs

Given the findings above, we have computed new epoch-dependant $V_{ss} = 6$ V PC and WT RMFs to account for the increase in spectral broadening and changing event threshold, at approximately 2 yearly intervals. The additional RMF broadening was achieved by increasing the electronic noise and CTI values input to the CCD Monte-Carlo simulator (described in previous release notes SWIFT-XRT-CALDB-09_v18 and SWIFT-XRT-CALDB-09_v17), as shown in table 1. The epoch dependent RMFs are listed in table P1.

Comparison with Calibration Sources

A number of astrophysical sources are used to regularly monitor the state of the XRT calibration and check the level of agreement seen between other X-ray observatories, some results when testing the broadened RMFs follow.

RX J1856.5–3754

The isolated neutron star RX J1856.5–3754 is considered to be a stable, soft X-ray source, modelled as a 63 eV blackbody (e.g. Beuermann et al., 2006, A&A, 458, 541). The source has been observed regularly since the substrate voltage changed in order to monitor the low energy response of the XRT. The relative normalisation of the model when applied to grade 0 data from different observational epochs and as a function of the lowest energy used in the fit is shown in figure 1.

For both modes, the relative normalisation shows $\sim 10 - 20$ percent variations with time when fitting the data down to 0.3 keV, with WT mode, in particular, showing a loss of low energy counts below ~ 0.4 keV at later epochs (see figure 2). The loss of low energy counts is related to the build up of charge traps within the CCD, as traps cause a significant fraction of charge from low energy X-rays to be lost below the event threshold, which is then not recoverable. For unabsorbed sources such as this, the effect can be alleviated by increasing the lowest energy used in the fit — for example, to 0.4 keV in 2013.

Note, however, that data taken after the WT event threshold changed (i.e. from 2013–Dec–12) show the WT spectrum of this soft source can be reliably used (and are well fit) down to 0.3 keV once more.

We further note that for soft sources such as this, small gain offsets of 10 – 20 eV can be responsible for 10 – 15 percent normalisation variations.

SNR 1E0102.2–7219

Observations of the line-rich source SNR 1E0102.2–7219 were used, along with its IACHEC reference model (Plucinsky et al., 2012, SPIE, 8443, 12), to verify that the intrinsic resolution of the response kernel match the data for different epochs in both PC and WT mode. Example spectra from different epochs, fit with the broadened RMFs, are shown in figure 3.

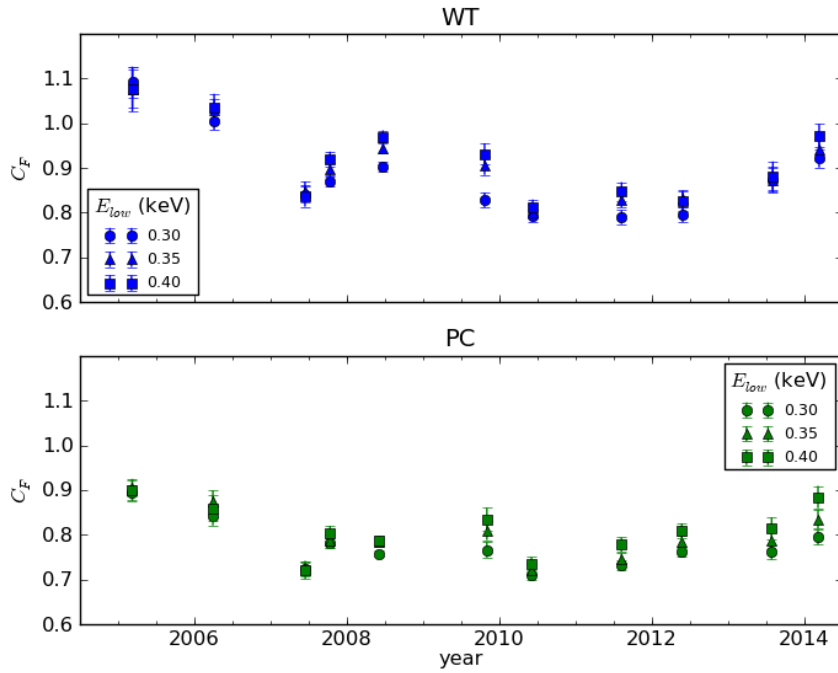


Figure 1: The relative blackbody normalisation obtained when fitting grade 0 WT (top) and PC (bottom) spectra of the soft NS RX J1856.5–3754 with a 63 eV blackbody (e.g. Beuermann et al., 2006, A&A, 458, 541), as a function of the fit lower energy (circles: 0.3 keV, triangles: 0.35 keV, squares: 0.4 keV).

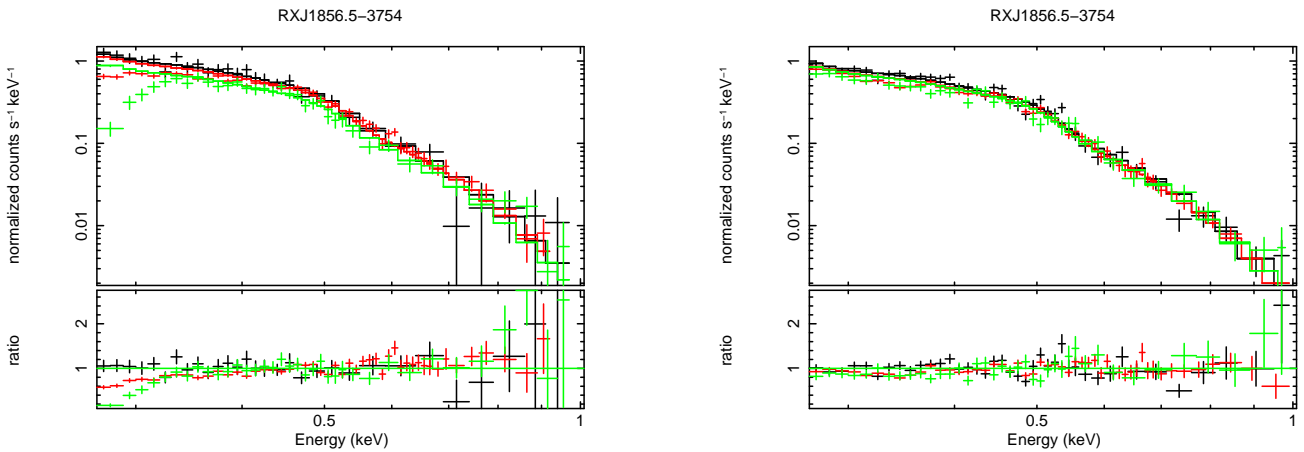


Figure 2: RX J1856.5–3754 WT (left) and PC (right) spectra (both grade 0) from 2005 (black), 2008 (red) and 2013 (green) and modelled with a 63 eV blackbody. The WT spectra show a drop-off in counts at the lowest energies with time due to the build-up of charge traps.

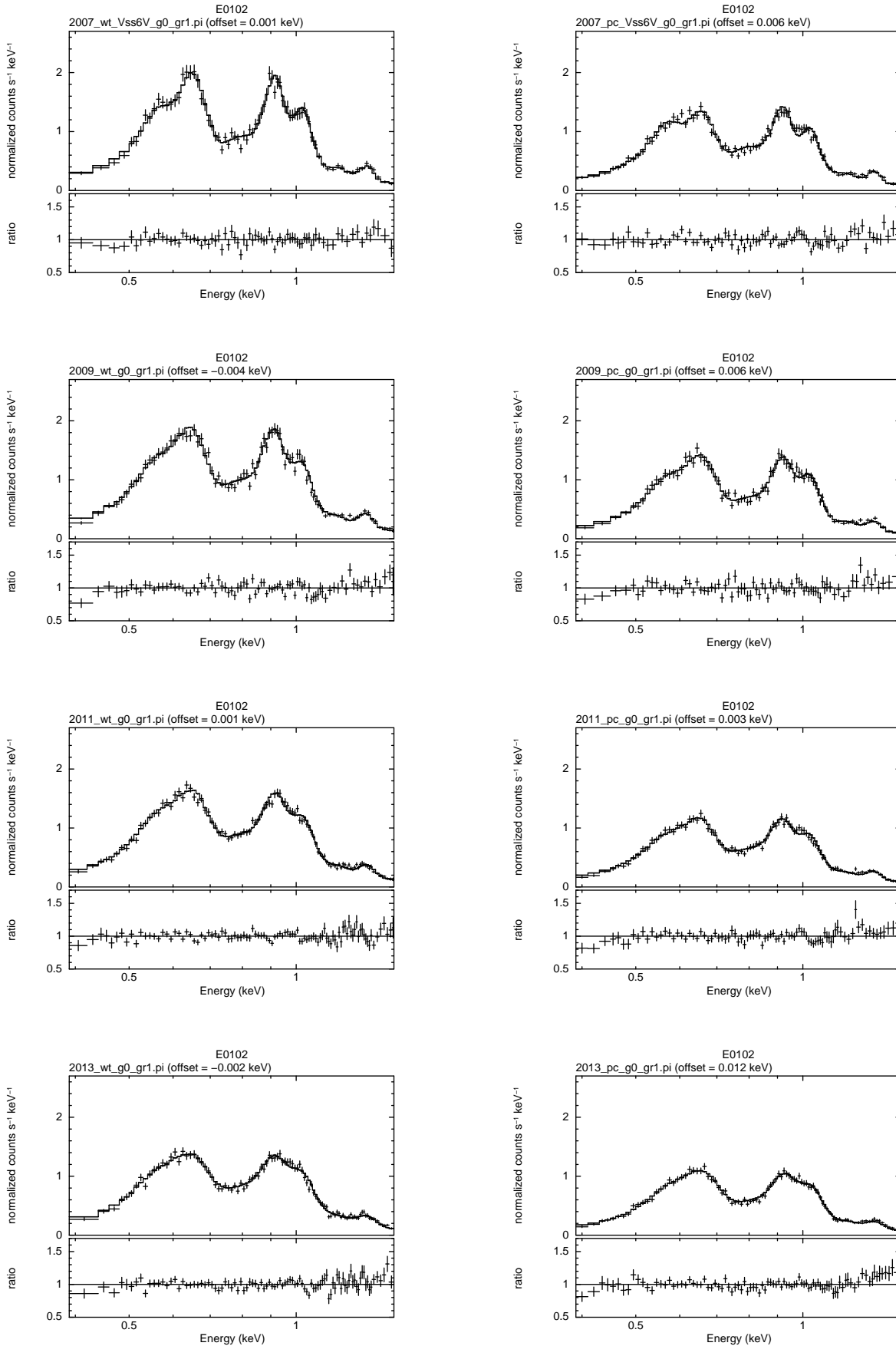


Figure 3: SNR 1E0102.2–7219 WT (left) and PC (right) spectra (both grade 0) from 2007, 2009, 2011, 2013 (top to bottom), modelled using the IACHEC reference model and the latest response files described in this document, illustrating the evolution of the spectral resolution at low energies and the good agreement between the observed and modelled resolution.

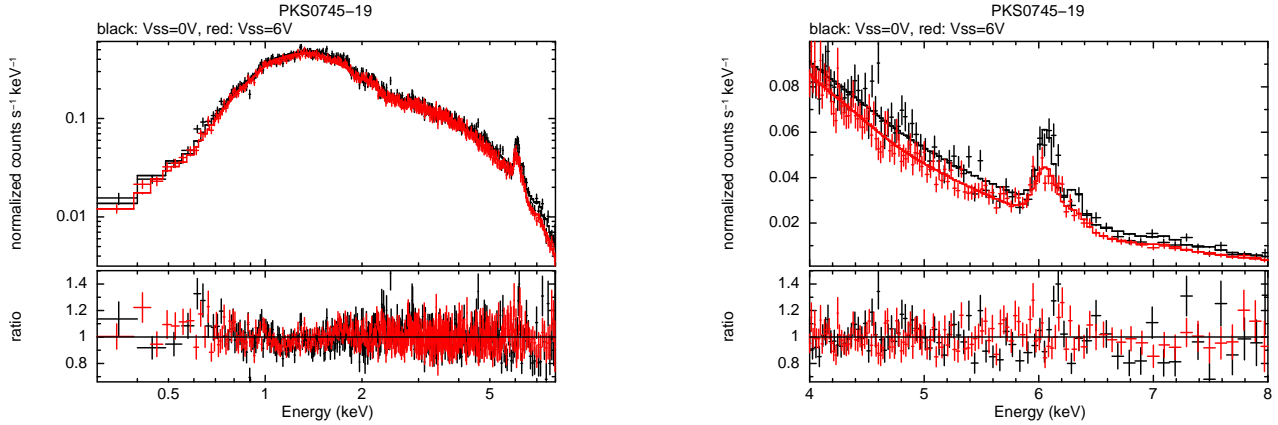


Figure 4: PC mode (grade 0–12) spectra from PKS 0745–19 showing the $V_{SS} = 0$ V epoch (2005) data in black and $V_{SS} = 6$ V epoch (2007–2012) data in red. The right panel shows a close-up view of the Fe-K α line region, illustrating the different level of broadening seen between the two epochs.

PKS 0745–19

The cluster of galaxies PKS 0745–19 was observed early in the mission (2005, exposure 57.7 ks), during the $V_{SS} = 0$ V era when the CCD instrumental resolution was at its best, and later a number of times after the substrate voltage was changed (2007 – 2012, exposure 115.9 ks). For both epochs, PC mode spectra were extracted from a region containing the central 90 arcsec of the cluster core. Data from the $V_{SS} = 6$ V interval were summed and an exposure weighted averaged RMF was constructed using the appropriate broadened RMF for each observation.

Figure 4 shows the observed broad-band PC mode spectra (fit with an absorbed thermal plasma [i.e. *apec*] model) and a close-up of the redshifted Fe-K α region. The latter illustrates the different level of instrumental broadening seen between the spectra and shows that the broadened RMF matches the data well at later times.

Current limitations and future prospects

Experience has shown that the RMF/ARFs described here can be used reliably over the energy range $0.3(0.4^1) - 10$ keV in PC mode and $0.3(0.4^1) - 10$ keV in WT mode and in general return fluxes which agree to within better than 10 per cent when compared with other X-ray missions.

The following considerations apply when using the RMFs/ARFs described here:

- The loss function, which is used by the simulator to describe how charge is incompletely collected from the X-ray interactions occurring near the surface of the device, shifts the redistribution peak of the lowest energy data down in energy. The loss function was derived from pre-launch laboratory calibration data obtained at the University of Leicester, using the central 200×200 pixel region of the detector, in order to be representative of XRT pointings taken close to the on-axis position. At the lowest input energies (C-K α at 0.277 keV; N-K α at 0.392 keV), the redistribution is seen to be non-uniform (see figure 5). If a source is positioned outside the central 200×200 region then it might show slightly worse redistribution than modelled by the RMF at the lowest energies (below ~ 0.4 keV).
- High signal-to-noise WT spectra from sources with featureless continua (such as Mrk 421) typically show residuals of about 3 per cent, for example, near the Au-M ν edge (at 2.205 keV), the Si-K edge (at 1.839 keV), or the O-K edge (at 0.545 keV). Occasionally, however, residuals nearer the 10 per cent level are seen, especially near the O-K edge, which are caused by small energy scale offsets (caused by inaccurate bias and/or gain corrections).

¹Depending on the epoch (see table 1).

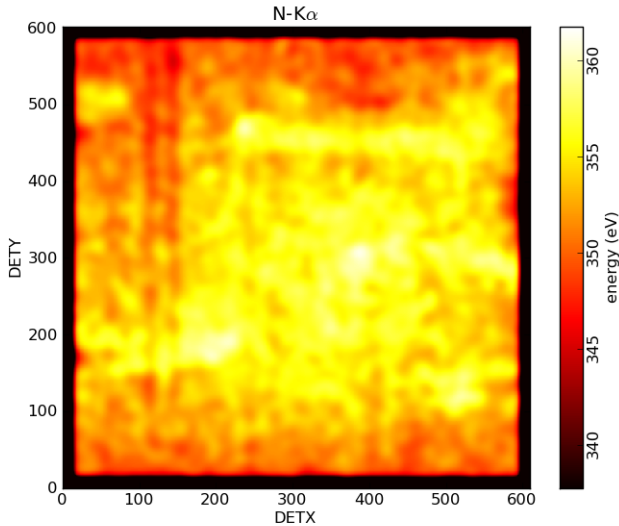


Figure 5: The spatial non-uniformity in the XRT spectral response over the surface of the detector at energies below ~ 0.4 keV is illustrated in this image which shows the average event energy for N-K α (0.392 keV) photons obtained from pre-launch laboratory calibration data. Event energy shifts of order 10 – 15 eV are visible outside the central 200×200 pixel region (from within which the response matrix loss function is calculated).

Data taken in PC mode can be similarly effected, though observations taken in this mode tend to have fewer counts and hence a lower statistical quality, which make the residuals less apparent.

Such residuals can often be improved through careful use of the *gain* command in XSPEC (by allowing the gain offset to vary by $\sim \pm 10 - 50$ eV).

- Also, observations of the soft NS RX J1856.5–3754 show that gain shifts of 10 – 20 eV can cause 10 – 15 per cent variations in the measured black-body normalisation.
- WT observations of absorbed point sources show CCD detector position dependent redistribution effects and are the subject of a supplementary WT RMF release.
- Note, while the epoch dependent files were generated with a certain range of dates in mind, our choice of date boundaries in making these RMFs reflects the continuous evolution of the CCD response, and does not relate to any quantised performance changes at these precise dates. Hence, if a source is observed either just before (or after) a given RMF starting date epoch (from table P1 or table A1) then it is possible the RMFs from the following (or preceeding) epoch will work equally well. ²
- A guide to the epoch dependant minimum energy to use when spectral fitting is included in table 1. The values, obtained by averaging data over multiple snapshots, are somewhat approximate, as the minimum energy depends on the effective threshold, which in turn depends on trap depths and locations, and can vary with the position of the source on the detector. It is possible that a specific snapshot of data could have a minimum usable energy higher (or lower) than those listed here, especially in WT mode (where the traps are deeper).

²The exception being the WT RMFs in use after the WT event threshold change on 2013-Dec-11.

Summary of RMFs/ARFs currently in use

The following table summarises the RMFs and ARFs available and recommended for XRT spectral analysis and their time dependence.

Table A1: *Swift*-XRT RMFs/ARFs in use as of 2014-Jun-10.

Observation Date		Mode	Grade	File names
From	To			
2004-Dec-01	2006-Dec-31	WT	0-2	swxwt0to2s0_20010101v012.rmf swxs0_20010101v001.arf
			0	swxwt0s0_20010101v012.rmf swxs0_20010101v001.arf
		PC	0-12	swxpc0to12s0_20010101v012.rmf swxs0_20010101v001.arf
			0-4	swxpc0to4s0_20010101v012.rmf swxs0_20010101v001.arf
			0	swxpc0s0_20010101v012.rmf swxs0_20010101v001.arf
		2007-Jan-01	2007-Aug-30	WT
0	swxwt0s0_20070101v012.rmf swxs0_20010101v001.arf			
PC	0-12			swxpc0to12s0_20070101v012.rmf swxs0_20010101v001.arf
	0-4			swxpc0to4s0_20070101v012.rmf swxs0_20010101v001.arf
	0			swxpc0s0_20070101v012.rmf swxs0_20010101v001.arf
Substrate voltage change from 0 V to 6 V on 2007-August-30				
2007-Aug-31	2008-Dec-31	WT	0-2	swxwt0to2s6_20010101v015.rmf swxs6_20010101v001.arf
			0	swxwt0s6_20010101v015.rmf swxs6_20010101v001.arf
		PC	0-12	swxpc0to12s6_20010101v014.rmf swxs6_20010101v001.arf
			0-4	swxpc0to4s6_20010101v014.rmf swxs6_20010101v001.arf
			0	swxpc0s6_20010101v014.rmf swxs6_20010101v001.arf
		2009-Jan-01	2010-Dec-31	WT
0	swxwt0s6_20090101v015.rmf swxs6_20010101v001.arf			
PC	0-12			swxpc0to12s6_20090101v014.rmf swxs6_20010101v001.arf
	0-4			swxpc0to4s6_20090101v014.rmf swxs6_20010101v001.arf
	0			swxpc0s6_20090101v014.rmf swxs6_20010101v001.arf

Table A1: continued.

2011-Jan-01	2012-Dec-31	WT	0-2	swxwt0to2s6_20110101v015.rmf swxs6_20010101v001.arf
			0	swxwt0s6_20110101v015.rmf swxs6_20010101v001.arf
		PC	0-12	swxpc0to12s6_20110101v014.rmf swxs6_20010101v001.arf
			0-4	swxpc0to4s6_20110101v014.rmf swxs6_20010101v001.arf
			0	swxpc0s6_20110101v014.rmf swxs6_20010101v001.arf
2013-Jan-01	2013-Dec-11	WT	0-2	swxwt0to2s6_20130101v015.rmf swxs6_20010101v001.arf
			0	swxwt0s6_20130101v015.rmf swxs6_20010101v001.arf
	Present	PC	0-12	swxpc0to12s6_20130101v014.rmf swxs6_20010101v001.arf
			0-4	swxpc0to4s6_20130101v014.rmf swxs6_20010101v001.arf
			0	swxpc0s6_20130101v014.rmf swxs6_20010101v001.arf
2013-Dec-12	Present	WT	0-2	swxwt0to2s6_20131212v015.rmf swxs6_20010101v001.arf
			0	swxwt0s6_20131212v015.rmf swxs6_20010101v001.arf

Note, the task XRTMKARF automatically reads in the correct ARF from the CALDB, based on information concerning the mode, grade and time of observation contained in the header of the input spectral file. The task also indicates to the screen which RMF is appropriate for the spectrum.

Useful Links

Summary of XRT RMF/ARF releases

XRT analysis threads at the UKSSDC, University of Leicester

XRT digest pages at the UKSSDC, University of Leicester

IACHEC website

http://www.swift.ac.uk/analysis/Gain_RMF_releases.html

<http://www.swift.ac.uk/analysis/xrt/>

<http://www.swift.ac.uk/analysis/xrt/digest.php>

<http://web.mit.edu/iachec/>